WiXus: A Wheeled-Legged Robot with Wire-Driven Environmental Utilizing to Integrate Mobility and Manipulation

Shintaro Inoue[1], Kento Kawaharazuka[1], Temma Suzuki[1], Sota Yuzaki[1], and Kei Okada[1]

***Abstract*— Wheeled-legged robots, which have wheels at their feet and achieve high mobility by coordinating wheel drive and leg drive, have been developed. These robots have been developed purely as platforms specialized for locomotion. Therefore, they do not have a means to repurpose their legs for roles other than locomotion, such as object manipulation or tool utilization. In this paper, we address the problem of how to draw out the potential task-execution capability of the legs by freeing them from the roles of locomotion through external body support. To this end, we propose and develop a new robot, WiXus, which fuses a wheeled-legged mechanism with a wire-driven mechanism that utilizes the external environment. The developed WiXus demonstrates not only planar locomotion with wheeled-legged drive, but also three-dimensional mobility such as cliff climbing by coordinating wire-driven and wheeled-legged actuation. Furthermore, by suspending the body with wire-driven actuation, WiXus successfully repurpose its legs as arms to perform object manipulation, (e.g., rescuing a dog (stuffed animal)), and tool utilization (e.g., harvesting an apple (mockup) with loppers). This study demonstrates that the approach of utilizing the environment with wire-driven actuation is a new design principle that extends the operational domain of wheeled-legged robots.**

I. Introduction

Wheeled-legged robots, which combine legged and wheeled actuation, have recently been studied and developed actively as locomotion platforms that achieve both high-speed locomotion on flat terrain and strong traversability on uneven terrain. In academic research, robots such as ANYmal on wheels [1], [2], SR600 [3], [4], and SUSTech-Nezha [5] have been developed. Furthermore, practical implementations by industry are also rapidly advancing, including Ascento [6], TITA [7], DIABOLO [8], Go2-W [9], and B2-W [10]. These developments indicate that wheeled-legged robots are already establishing their position as one of the completed forms of ground locomotion robots.

The high mobility of these robots comes from the ability to switch between the advantages of legs and wheels depending on the situation. On flat ground, they perform energy-efficient high-speed locomotion with wheels, while when encountering obstacles such as steps or rubble, they function as legs to traverse various terrains efficiently and stably. Based on this excellent locomotion capability, wheeled-legged robots with manipulators have emerged, such as Handle [11], which performs logistics tasks, and humanoid-type wheeled-legged robots with dual arms aiming for versatile operations [12], [13]. However, even these robots [11]–[13] fundamentally depend on the stability and driving force provided by having their legs or wheels in contact with the ground. Therefore, high places unreachable by legs, cliffs, and vertical walls remain outside their operational domain.

Fig. 1. Overview of WiXus, a robot that fuses a wheeled-legged system with a wire-driven system that anchors to the environment.

In contrast, to tackle the challenge of tasks in large three-dimensional spaces, an entirely different class of robots, wire-driven robots, has been studied. Cable-Driven Parallel Robots (CDPRs), which use wires deployed from fixed frames to actuate end-effectors, can support heavy loads with high precision in vast workspaces, and have applications such as CoGiRo [14], which mounts a manipulator, and SkyCam [15], which moves cameras in stadiums. More recently, this approach has evolved further, with research that utilizes the external environment itself, such as poles and trees, as the support base instead of relying on fixed frames. For example, there are studies where tethered drones serve as anchors to improve the traversability of ground vehicles [16], as well as CubiX [17], [18], a portable wire-driven robot that autonomously anchors wires to surrounding structures.

In this study, we propose a new approach that fuses wheeled-legged system and wire-driven system. Specifically, while using the high ground mobility of a wheeled-legged robot as the foundation, we augment it with the ability to reach areas that were previously outside the operational domain, such as high places, cliffs, and vertical walls, by utilizing the environment through wire anchoring. Furthermore,

[1] The authors are with the Department of Mechano-Informatics, Graduate School of Information Science and Technology, The University of Tokyo, 7-3-1 Hongo, Bunkyo-ku, Tokyo, 113-8656, Japan. [s-inoue, kawaharazuka, t-suzuki, yuzaki, k-okada]@jsk.imi.i.u-tokyo.ac.jp

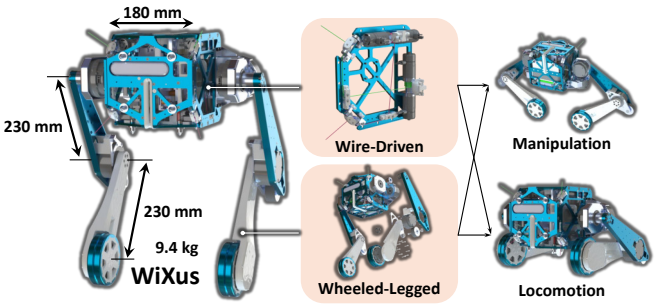

Fig. 2. Hardware overview of WiXus. It has a 180 mm cubic main body with modules for its wire-driven system and two attached wheeled-legs. These components work together to achieve both manipulation and locomotion.

by suspending the body with wire-driven actuation, the legs are freed from locomotion, and can be repurposed as arms for object manipulation and tool utilization. To embody this concept, we propose WiXus, shown in Fig. 1, and demonstrate its design and capabilities. WiXus represents a novel attempt to integrate environmental utilization by wire-driven actuation into a wheeled-legged robot, achieving tasks that were previously difficult, such as cliff climbing, manipulation while floating, and tool utilization. The proposed approach of utilizing the environment has the potential to extend to real-world applications such as outdoor operations, disaster response, and agriculture, and thus has practical significance beyond laboratory demonstrations.

II. Design of WiXus

A. Overall Design

An overview of the design of WiXus is shown in Fig. 2. WiXus consists of a main body equipped with wire winding modules, and two wheeled-legs each with a 3-DOF (Roll-Pitch-Pitch) leg and an attached wheel. By integrating wire-driven actuation with the wheeled-legs, WiXus enhances both its object manipulation capability and locomotion capability.

The main body is a cube with dimensions of 180 mm on each side, and four wires can be deployed from its front vertices. By anchoring these wires to surrounding structures in the environment and winding them, the robot can drive itself. In addition, one more wire can be deployed from the center of the rear side, which enables the robot to attach tools to its body.

The two wheeled-legs are attached to the left and right sides of the main body. In addition to performing locomotion with legs and wheels, they also function as manipulators when the robot is suspended by the wire-driven system. During manipulation, the main body is rotated by -90 degrees in the pitch direction, which gives the legs 3 DOFs (Yaw-Pitch-Pitch) as arms.

B. Wheeled-Leg Design

The structure of the designed wheeled-leg is shown in Fig. 3. Each wheeled-leg consists of a Hip-Link, a Thigh-Link, a Calf-Link, and a wheel. The joint configuration from the Base-Link to the Calf-Link follows the Roll-Pitch-Pitch arrangement, which is the same as in typical wheeled-legged

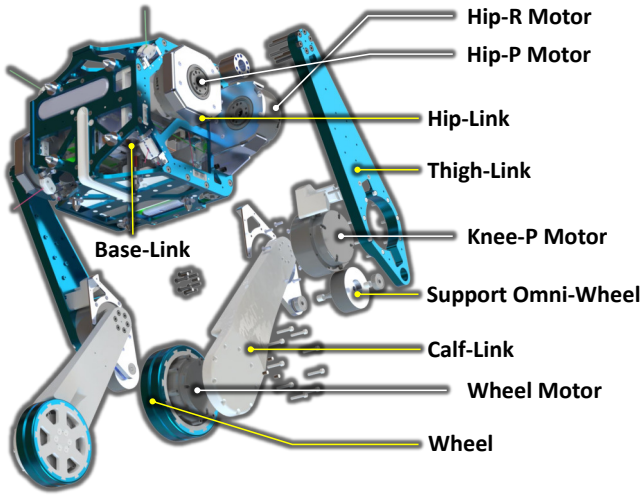

Fig. 3. Overview of the wheeled-leg design. It consists of a 3-DOF leg with a Roll-Pitch-Pitch joint configuration, a wheel mounted at its tip, and a support omni-wheel at the knee.

robots [6]–[10]. While these robots [6]–[10] use linkage mechanisms to transmit the elbow joint rotation in order to reduce the weight of the leg tip, WiXus directly mounts motors on the elbow joints to maximize the leg workspace. Robstride02 actuators were adopted for the joints because of their high power density, and smaller CyberGear actuators of the same family were used for the wheels.

The lengths of the Thigh-Link and Calf-Link are 230 mm each. This was determined as 80% of the self-supportable leg length calculated from the maximum continuous torque of the actuators and the mass of the robot.

An omni-wheel is attached to the Thigh-Link as a support wheel, enabling stable two-wheeled driving with the elbows in contact with the ground (as shown in the lower right of Fig. 2).

The Calf-Links and wheels were manufactured using a 3D printer, while the other links were made from machined aluminum parts. For the filament of the 3D-printed parts, POTICON (Potassium Titanate Compound) NTL34M, a high-strength plastic, was used. For the wheels, 3D-printed TPU (Thermoplastic Polyurethane) parts with a fuzzy skin covering their outer surface were fitted to increase the friction coefficient against the ground and manipulated objects.

C. Wire Winding Module Design

The arrangement of the wires and wire winding modules of WiXus is shown in Fig. 4. WiXus can wind a total of five wires: four wires for anchoring to the environment and one wire for attaching tools.

The wires for environmental anchoring originate from each front vertex (Fig. 4①–④). Each wire is wound by one of the wire winding modules installed in pairs on the left and right sides. The wires at Fig. 4① and ③ correspond to the left-side modules, and those at ② and ④ correspond to the right-side modules. Fig. 5 (left) shows the detailed structure of the side modules. Each wire winding module consists of a winch that winds the wire, two motors that

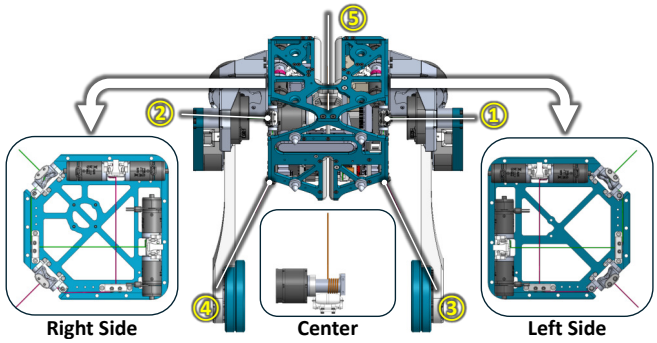

Fig. 4. Arrangement of the wire winding modules on the main body. WiXus is equipped with a total of five modules: four modules for environmental anchoring are mounted on the sides, while a single module for tool attachment is located at the center.

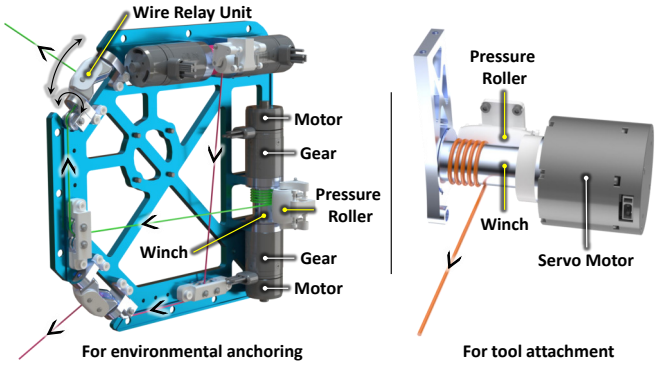

Fig. 5. Overall structure of the two types of wire winding modules: one for environmental anchoring and one for tool attachment. A motor drives a winch to wind the wire.

rotate the winch, and a pressing roller that holds the wire in place. The winch has a diameter of 15 mm and a width of 21.5 mm, and it is rotated by two motors mounted on both sides. M2006 motors, which are cylindrical and controllable via CAN communication, were adopted. The pressing roller keeps the wound wire aligned on the winch by pressing it with spring tension. Each wire is guided along the edge of the side surface through low-friction pulleys to avoid interference with other wires and components, and exits the robot through a wire relay unit. The wire relay unit allows the wire to be routed in any direction around its origin. This structure is symmetrically installed on the left and right sides. The maximum continuous tension is about 120 N, and the maximum winding length is about 6 m. The wires are made of Vectran®, a high-performance rope of about 1.0 mm diameter made from high-strength polyarylate fiber.

The wire for tool attachment originates from the groove at the center of the rear side (Fig. 4⑤). It is wound by a wire winding module mounted at the center, whose details are shown in Fig. 5 (right). This wire winding module consists of a servo motor, a winch, and a pressing roller. The winch has a diameter of 22 mm and a width of 40 mm, and a small Robstride00 actuator of the same family as the joint actuators was adopted as the servo motor. The maximum continuous tension is about 420 N, and the maximum winding length is about 6 m. The wire is made of Dyneema®, which has a higher strength than the environmental anchoring wires and a diameter of about 2.0 mm.

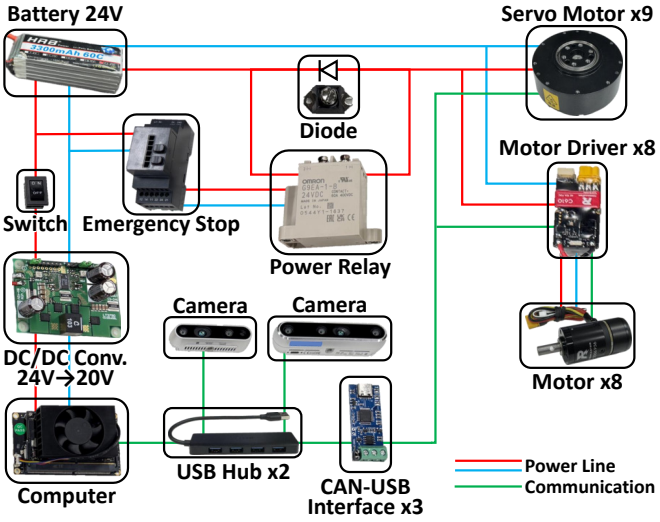

Fig. 6. Circuit configuration of WiXus. A total of 17 motors (eight for the wheeled-legs and nine for the wire-driven system) are controlled by a computer via three CAN-USB interfaces. The system also includes two RGB-D cameras with onboard IMUs.

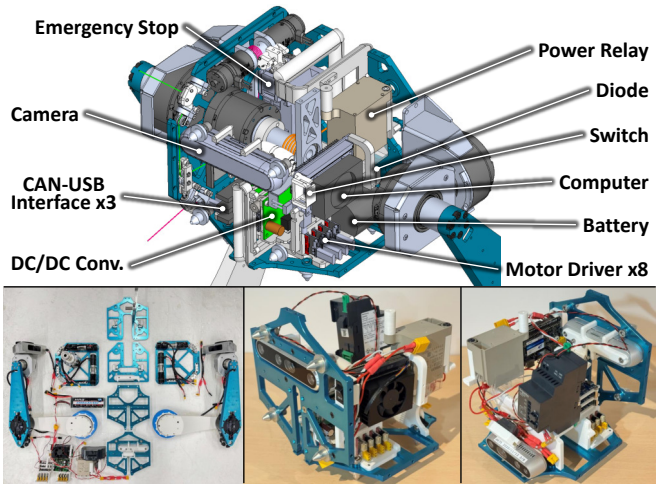

Fig. 7. Layout of the electronic components. The components are housed within the main body, arranged to prevent any interference with the wires.

D. Onboard Circuits and Architecture

The circuit configuration of WiXus is shown in Fig. 6. A 24 V battery is connected to the computer (Jetson Orin Nano) through a power switch and a DCDC converter. Two cameras (Intel RealSense D455 and D435i) and three CAN-USB interfaces are connected to the computer via two USB hubs. The D435i is not used in this study. The computer communicates with each servo motor and motor driver through the CAN-USB interfaces. The same battery also powers the motors through a power relay. The power relay is controlled by a wireless emergency stop system, which allows the robot to be remotely stopped in case of abnormal behavior during experiments. In addition, a current path with a diode is implemented to allow regenerative current from the motors to flow back to the battery. Note that the motors for the joints, wheels, and tool attachment are servo motors with integrated motor drivers.

As shown in the upper part of Fig. 7, these circuit components are placed inside the robot without interfering

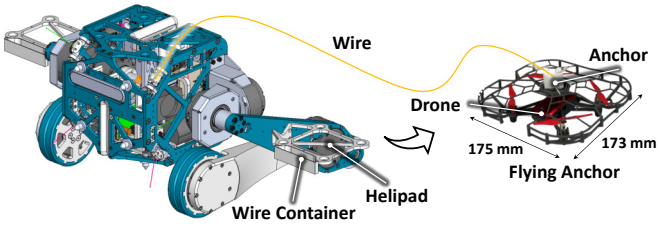

Fig. 8. The flying anchor, a custom drone for autonomous wire anchoring to the environment. Attached to the tip of the wire, this module combines a drone with an anchor.

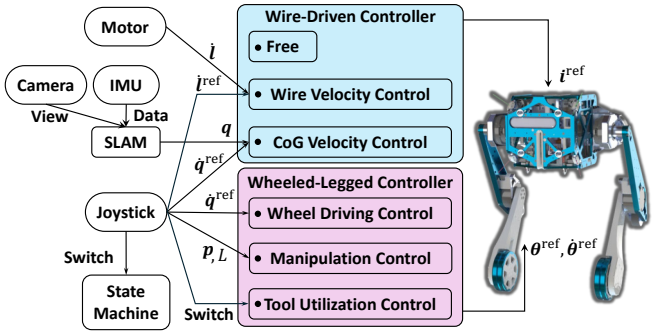

Fig. 9. The software architecture of WiXus. The system features two main control modules that operate in parallel: a wire-driven controller and a wheeled-legged controller.

with the wires. This circuit configuration is implemented in the actual robot as shown in the lower part of Fig. 7. Fig. 7 (lower left) shows the fully disassembled robot laid out, and Fig. 7 (lower right) shows only the assembled portion around the circuit components.

E. Optional Sub-Module: Flying Anchor

As a method for autonomously anchoring wires to the environment, the flying anchor [17] has been proposed. WiXus can also autonomously anchor its wires to the environment using the flying anchor. As shown in Fig. 8, the flying anchor consists of an anchor attached to the tip of a wire and a drone. After the flying anchor flies around the target structure to wrap the wire around it, winding the wire secures the anchor in place. When using the flying anchor to anchor a wire to the environment, wire containers and helipads are mounted on both legs. The wire container stores the wire that has been previously unwound from the winch and bundled, and the helipad serves as a launch pad for the flying anchor.

As in the method for controlling the flying anchor using an RGB-D camera [19], the flying anchor is autonomously controlled by WiXus itself while being observed by WiXus's camera (D455).

III. Controller and System of WiXus

A. Control System Architecture

The system architecture of WiXus is shown in Fig. 9. Two types of controllers—the wire-driven controller and the wheeled-legged controller—are executed in parallel, constantly controlling all actuators. In addition, RTAB-Map [20] for SLAM is running separately using the D455 camera. Furthermore, a state machine implemented with SMACH [21] is used to manage the mode transitions of the two controllers. Command inputs to each controller and mode

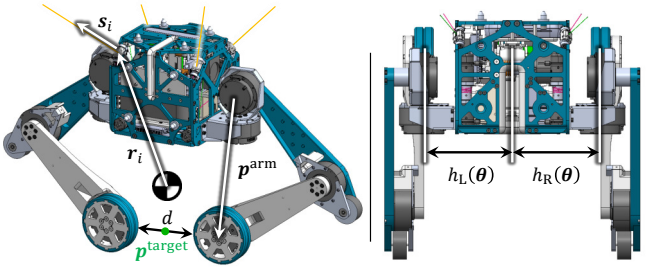

Fig. 10. Definition of symbols used in the wire-driven, manipulation, and wheeled locomotion controllers.

switching are performed through joysticks (Sony DualSense and 3Dconnexion SpaceNavigator).

B. Wire-Driven Control

The wire-driven controller has three modes: *free*, *wire velocity control*, and *center-of-gravity (CoG) velocity control*, and it controls the wires anchored to the environment.

In the *free* mode, each motor of the wire winding modules is always commanded with a current of 0 A. This mode is activated when only locomotion by the wheeled-legs is performed and wire-driven actuation is not used.

In the *wire velocity control* mode, the target wire velocity $\dot{\boldsymbol{l}}$ is given as input. The controller computes and outputs the target tensions $\boldsymbol{f}^{\mathrm{ref}}$ using P control so that the actual wire velocities $\dot{\boldsymbol{l}}$ approach the targets while compensating for gravity. If the number of wires anchored to the environment is m, the target tension f_i^{ref} of the i-th wire is calculated as:

$$f_i^{\mathrm{ref}} = \frac{M\|\boldsymbol{g}\|}{m} + K_p\left(\dot{l}_i - \dot{l}_i^{\mathrm{ref}}\right) \tag{1}$$

where M is the mass of the robot, $\boldsymbol{g}$ is the gravitational acceleration vector, and K_p is the proportional gain. Because this control distributes the gravity compensation tension equally to each wire, it does not require the robot's posture information, but it is only useful when the wires are nearly vertical.

In the *CoG velocity control* mode, the target CoG velocity $\dot{\boldsymbol{q}}^{\mathrm{ref}}$ is given as input. The controller computes and outputs the target tensions $\boldsymbol{f}^{\mathrm{ref}}$ so that the robot follows the target while compensating for gravity, as:

$$\boldsymbol{f}^{\mathrm{ref}} = \boldsymbol{f}^{g} + K_p\left(\dot{\boldsymbol{l}} + \boldsymbol{W}^{\top}(\boldsymbol{q})\dot{\boldsymbol{q}}^{\mathrm{ref}}\right) \tag{2}$$

Here, $\boldsymbol{W}(\boldsymbol{q})$ is a $6\times m$ Jacobian matrix expressed using the position vector $\boldsymbol{r}_i$ of the wire origin and the unit direction vector $\boldsymbol{s}_i$ (as shown in Fig. 10 left):

$$\boldsymbol{W}(\boldsymbol{q}) = \begin{bmatrix} \boldsymbol{s}_1 & \cdots & \boldsymbol{s}_m \\ \boldsymbol{r}_1\times\boldsymbol{s}_1 & \cdots & \boldsymbol{r}_m\times\boldsymbol{s}_m \end{bmatrix} \tag{3}$$

The first term of Eq. 2 is the gravity compensation term $\boldsymbol{f}^{g}$, computed by solving the following quadratic programming problem:

$$\begin{aligned} \min_{\boldsymbol{f}^{\mathrm{g}}} \quad & \|\boldsymbol{W}(\boldsymbol{q})\boldsymbol{f}^{\mathrm{g}} - M\boldsymbol{g}\|^2 \\ \text{s.t.} \quad & \boldsymbol{f}^{\min} \le \boldsymbol{f}^{\mathrm{g}} \le \boldsymbol{f}^{\max} \end{aligned} \tag{4}$$

where $\boldsymbol{f}^{\min}, \boldsymbol{f}^{\max}$ are the minimum and maximum tension limits. The second term of Eq. 2 is the CoG velocity tracking

term, which converts the target CoG velocity $\dot{\boldsymbol{q}}^{\text{ref}}$ to the target wire velocity using the Jacobian $\boldsymbol{W}(\boldsymbol{q})$, and applies P control so that the actual wire velocity $\dot{\boldsymbol{l}}$ follows it. All tensions and wire velocities are represented as m-dimensional vectors for the m anchored wires.

The motors (M2006) used in the anchoring wire winding modules are small and have gearheads with a reduction ratio of 36:1, which causes friction effects during control. Therefore, the computed tensions are converted into current commands $\boldsymbol{i}^{\text{ref}}$ with compensation for both Coulomb friction and load-dependent friction as:

$$\boldsymbol{i}^{\text{ref}} = r\boldsymbol{K}_{\boldsymbol{t}}^{-1}\boldsymbol{f}^{\text{ref}} + \boldsymbol{i}_{\boldsymbol{0}} + \boldsymbol{i}_{\boldsymbol{L}}\frac{\|\boldsymbol{f}^{\text{ref}}\|}{M\|\boldsymbol{g}\|} \tag{5}$$

where r is the winch radius, $\boldsymbol{K}_{\boldsymbol{t}}$ is a diagonal matrix of motor torque constants, $\boldsymbol{i}_{\boldsymbol{0}}$ is the Coulomb friction compensation current, and $\boldsymbol{i}_{\boldsymbol{L}}$ is the load-dependent friction coefficient. $\boldsymbol{i}_{\boldsymbol{0}}$, $\boldsymbol{i}_{\boldsymbol{L}}$, and $\boldsymbol{K}_{\boldsymbol{t}}$ are identified from static current measurements under no-load and suspended conditions, based on the balance of friction and gravity (details omitted due to space).

Each anchoring wire winding module has two motors per winch, which are controlled as one motor by applying the same magnitude currents with opposite signs.

C. Wheeled-Legged Control

The wheeled-legged controller has three modes: *wheel driving control*, *manipulation control*, and *tool utilization control*.

In the *wheel driving control* mode, when the robot takes a vehicle form with its wheels and support wheels contacting the ground, the controller outputs the target wheel angular velocities $\dot{\theta}^{\text{ref}}_{\text{L wheel}}$, $\dot{\theta}^{\text{ref}}_{\text{R wheel}}$ that track the target translational velocity $\dot{q}_x^{\text{ref}}$ and the target yaw angular velocity $\dot{q}^{\text{ref}}_{\text{yaw}}$, as:

$$\begin{aligned}\dot{\theta}^{\text{ref}}_{\text{L wheel}} &= \frac{\dot{q}_x^{\text{ref}} - \dot{q}^{\text{ref}}_{\text{yaw}} h_{\text{L}}(\boldsymbol{\theta})}{R} \\ \dot{\theta}^{\text{ref}}_{\text{R wheel}} &= \frac{\dot{q}_x^{\text{ref}} + \dot{q}^{\text{ref}}_{\text{yaw}} h_{\text{R}}(\boldsymbol{\theta})}{R}\end{aligned} \tag{6}$$

where R is the wheel radius and $h_{\text{L,R}}(\boldsymbol{\theta})$ is the distance from the robot center to each wheel, as shown in Fig. 10 (right). The target joint angles $\boldsymbol{\theta}^{\text{ref}}$ of the other joints are fixed in the vehicle posture, except for the Hip-P joint, which can be operated to change the pitch angle of the Base-Link.

In the *manipulation control* mode, as shown in Fig. 10 (left), both wheeled-legs grasp and manipulate the target object. The inputs are the target position $\boldsymbol{p}^{\text{target}}$ between the wheels and the width d (shown in Fig. 10 left). Only the Hip-P joint angle $\theta_{\text{Hip-P}}$ and the Knee-P joint angle $\theta_{\text{Knee-P}}$ are controlled, and the two leg tips always move on the same plane. In this configuration, each wheeled-leg behaves as a typical 2-DOF arm, and their target joint angles can be computed analytically by solving the inverse kinematics as:

$$\begin{aligned}\theta^{\text{ref}}_{\text{Knee-P}} &= \arccos\frac{\|\boldsymbol{p}^{\text{arm}}\|^2 - L^2_{\text{thigh}} - L^2_{\text{calf}}}{2L_{\text{thigh}}L_{\text{calf}}} \\ \theta^{\text{ref}}_{\text{Hip-P}} &= \arctan\frac{\boldsymbol{p}^{\text{arm}}_y}{\boldsymbol{p}^{\text{arm}}_x} - \arctan\frac{L_{\text{calf}}\sin\theta^{\text{ref}}_{\text{Knee-P}}}{L_{\text{thigh}} + L_{\text{calf}}\cos\theta^{\text{ref}}_{\text{Knee-P}}}\end{aligned} \tag{7}$$

where $\boldsymbol{p}^{\text{arm}}$ is the target tip position vector geometrically calculated from $\boldsymbol{p}^{\text{target}}$, d, and R, and L_{thigh} and L_{calf} are the link lengths shown in Fig. 10 (left). In addition, the wheel angular velocities can also be controlled to lift the object by rotating the wheels when grasping it with the wheels.

In the *tool utilization control* mode, the controller outputs the target joint angles $\boldsymbol{\theta}^{\text{ref}}$ of the wheeled-legs for using the tool. For example, in the tool utilization experiment described in Subsection IV-C, loppers are used. Using the loppers requires opening and closing motions. The joint angles when opening and closing the loppers with the wheeled-legs are recorded in advance, and the controller switches between these joint angles to achieve the tool utilization.

IV. Experiments

A. Mobility Capabilities

To demonstrate the mobility capabilities of WiXus, we conducted the following two experiments.

1) Planar Mobility and Mapping: In this experiment, WiXus creates a map while moving on a flat surface using its wheels. As shown in Fig. 11, WiXus builds a map of the surrounding environment and estimates its own position and velocity using RTAB-Map [20] with the D455 camera while moving on wheels. Here, the wire-driven controller is in the *free* mode, and the wheeled-legged controller is in the *wheel driving control* mode. In addition, as shown in Fig. 11③, the pitch angle of the Base-Link is changed, which also changes the pitch direction of the camera's field of view used for SLAM.

Looking at Fig. 12, the translational velocity q_x is achieved as commanded through the wheel velocities $\dot{\theta}_{\text{L wheel}}$, $\dot{\theta}_{\text{R wheel}}$. Although there is some error in the rotational velocity q_{yaw}, considering that q_y (which should be 0 m/s) is not zero, it is likely due to estimation errors in the SLAM system. In this study, the self-localization uses only the RGB-D images and IMU sensor data from the D455, but incorporating wheel velocity or wire velocity measurements could lead to more stable estimation.

For a robot driven by anchoring wires to the environment, observing and recording the environment is an important preparatory task, and this experiment shows that WiXus can perform it by itself. In the experiments in Subsection IV-B and Subsection IV-C, the environments to which the wires are anchored are assumed to be known in advance, and this prior information is obtained by WiXus itself through such observation and recording.

2) Three-Dimensional Mobility: Cliff Climbing: In this experiment, WiXus climbs a cliff by combining wire-driven actuation and wheeled-legged locomotion. As shown in Fig. 13, WiXus anchors two wires to a tree branch located above the cliff and winds them up to climb while driving its wheels along the cliff surface. Here, the wire-driven controller is in the *wire velocity control* mode, and the wheeled-legged controller is in the *wheel driving control* mode.

Looking at Fig. 14, the decrease in the wire lengths l_1, l_2 together with the wheel velocities $\dot{\theta}_{\text{L wheel}}$, $\dot{\theta}_{\text{R wheel}}$ indicates

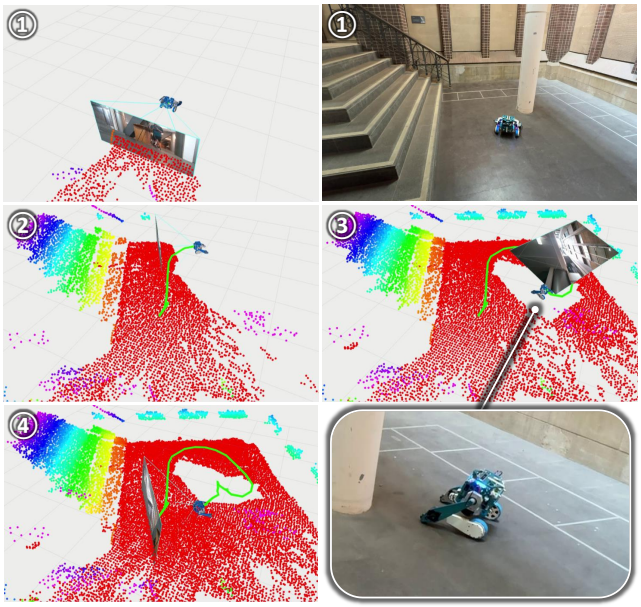

Fig. 11. Scenes from the planar mobility and mapping experiment. WiXus can generate a map while performing wheeled locomotion and controlling the pitch angle of its main body.

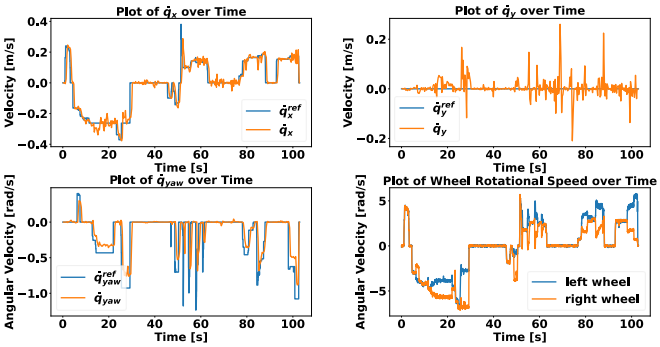

Fig. 12. Time-series data of the velocity and actual wheel speeds during mapping. The wheel speeds are calculated to track the commanded velocity.

that WiXus climbs the cliff by coordinating wire-driven actuation and wheeled-legged locomotion. Focusing on the wire velocities $\dot{l}_1, \dot{l}_2$, they track the target values with oscillations. This is considered to be caused by the insufficient control frequency of the velocity P control. The M2006 motors used for the wire-driven actuation are designed to receive current commands as control inputs. Therefore, the P control is executed on WiXus's onboard computer, resulting in a lower control frequency. Since the wire lengths do not oscillate, this does not affect the behavior in this experiment, but for more precise tasks, high-frequency feedback control on the motor driver board with servo motors would be desirable.

B. Object Manipulation: A Rescue Task

In this experiment, WiXus performs a rescue-like task to demonstrate its object manipulation capability, lifting and transporting a dog (a stuffed animal) to a safe location. In this task, two flying anchors are used to autonomously anchor two wires to the environment, also demonstrating that WiXus can autonomously anchor wires to the environment.

As shown in Fig. 15①, the goal of this task is to carry the dog into the basket. A ceiling-mounted frame marked with

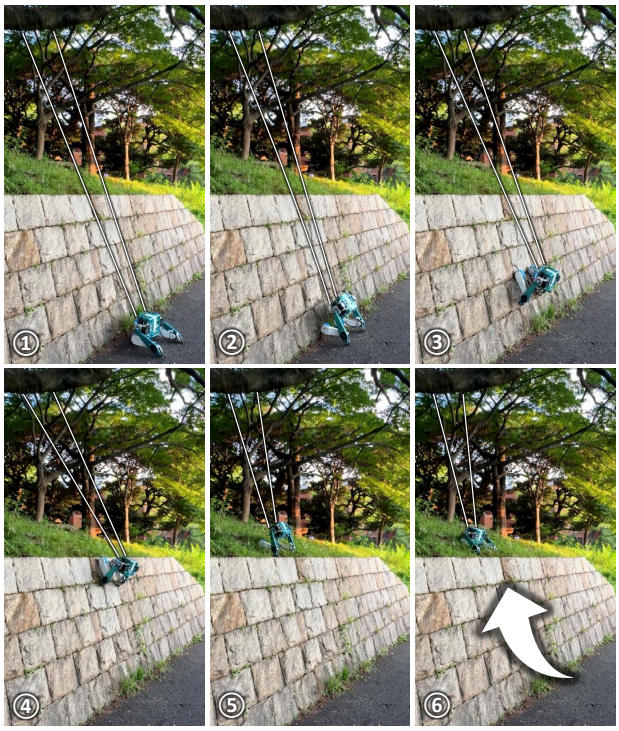

Fig. 13. Scenes from the cliff climbing experiment. WiXus successfully climbs the cliff by coordinating its two wheeled-legs with two wires anchored to the environment.

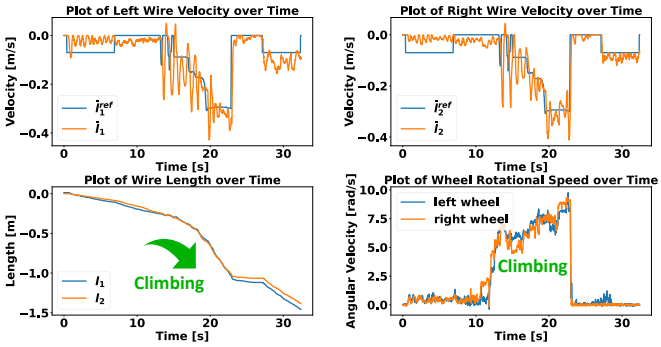

Fig. 14. Time-series data of wire velocity, wire length, and wheel speeds. The data shows that the wire winding and wheel drive systems are actuated simultaneously.

red circles is available for wire anchoring. At first, the wire-driven controller is in the *free* mode and the wheeled-legged controller is in the *wheel driving control* mode. In Fig. 15②–⑥, the flying anchors fly around using the RGB-D camera-based control method [19] and autonomously anchor the wires to the environment. In Fig. 15⑦, WiXus suspends itself by wire-driven actuation, and in Fig. 15⑧, it changes its joint angles to take a posture suitable for object manipulation. Here, the wire-driven controller is switched to the *CoG velocity control* mode, and the wheeled-legged controller is switched to the *manipulation control* mode. In Fig. 15⑨–⑮, WiXus grasps the dog with its wheeled-legs and transports it to the basket by moving through space while suspended by the wires.

As shown in Fig. 16, the two flying anchors anchor the wires to the environment by flying around the frame, and WiXus moves through space while suspended.

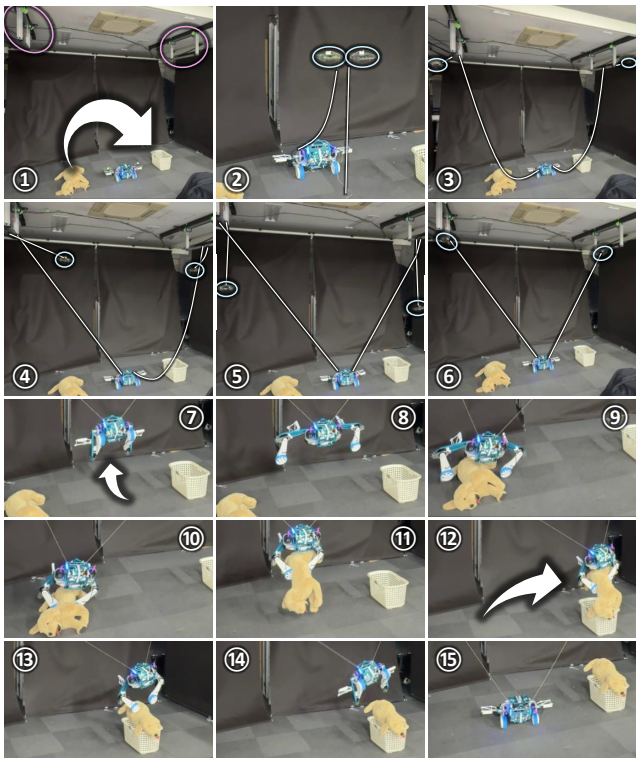

Fig. 15. Scenes from the rescue task experiment. Two Flying Anchors autonomously anchor two wires to the environment, enabling WiXus to move the space using the wires. Subsequently, the robot manipulates and transfers a dog using its wheeled-legs.

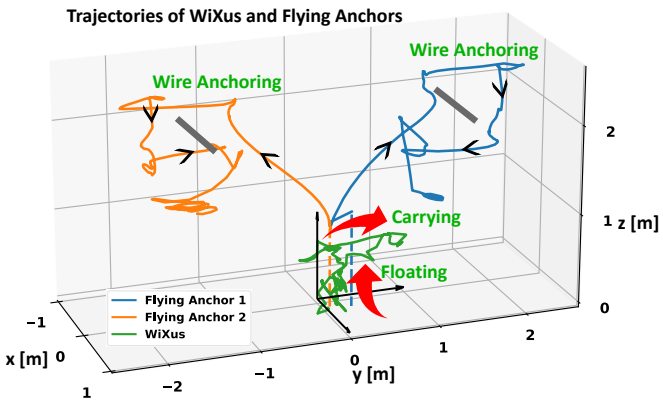

Fig. 16. The trajectories of the two Flying Anchors and WiXus. This figure shows the paths of the Flying Anchors as they anchor the wires to the environment, and the resulting trajectory of WiXus as it moves through the space.

This experiment demonstrates the unique capability of combining wire-driven actuation and wheeled-legged locomotion, where the wheeled-legs become arms when WiXus is suspended by the wires, enabling object manipulation. Furthermore, the entire sequence from wire anchoring to object manipulation operates seamlessly, showing the high task execution capability of WiXus.

C. Tool Utilization: Harvesting with Loppers

In this experiment, WiXus performs a harvesting-like task using a tool to demonstrate its ability to execute tasks with tools. It uses loppers to cut apples from a tree.

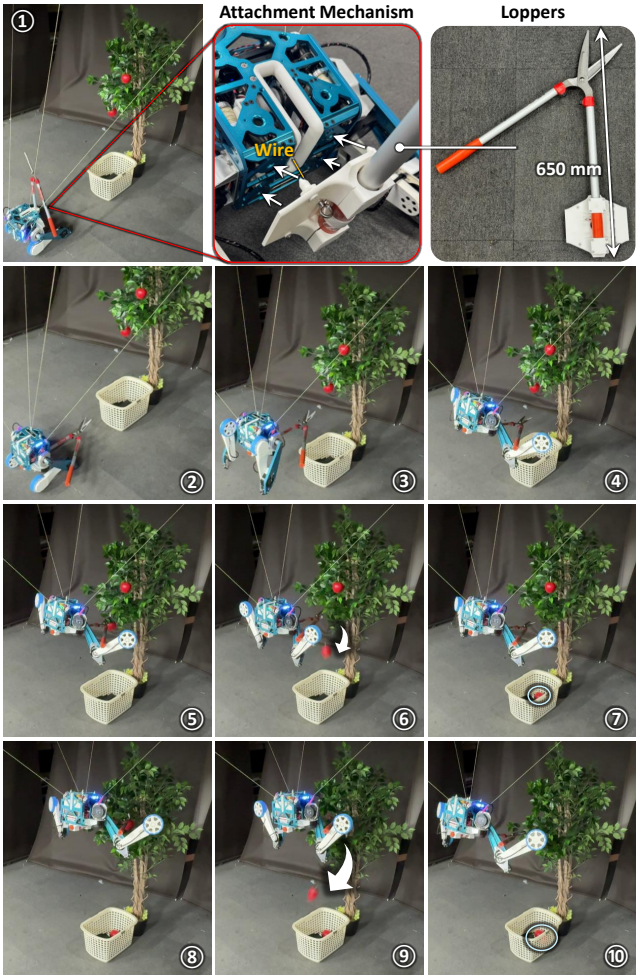

Fig. 17. The tool attachment mechanism for the loppers and scenes from the apple harvesting task experiment. WiXus moves to the target apple using its wire-drive, and then uses its wheeled-legs to actuate the loppers and perform the harvest.

As shown in Fig. 17①, the experiment is conducted with four wires anchored to the environment. WiXus attaches a 650 mm long pair of loppers to its body using the tool attachment wire. The faces of the Base-Link have uneven surfaces, which fit into the matching shape of the fixture attached to the loppers to hold them in place. The loppers are secured to the body by keeping tension on the tool attachment wire. In Fig. 17②–④, WiXus suspends itself with the wire-driven actuation and changes the joint angles of its wheeled-legs to take a posture for operating the loppers. Here, the wire-driven controller is in the *CoG velocity control* mode, and the wheeled-legged controller is in the *tool utilization control* mode. In Fig. 17⑤–⑦, WiXus moves through space using the wire-driven actuation to reach an apple, and closes and opens the loppers with its wheeled-legs to harvest an apple. In Fig. 17⑧–⑩, it similarly harvests a second apple.

In this experiment, an operator controls the target CoG velocity of WiXus while observing the apples and the loppers. As seen in Fig. 18, the target CoG velocities $q_x^{\mathrm{ref}}, q_y^{\mathrm{ref}}, q_z^{\mathrm{ref}}$ are not smooth, showing that WiXus is finely maneuvered.

The loppers used in this experiment require not only controlling their orientation but also switching their state

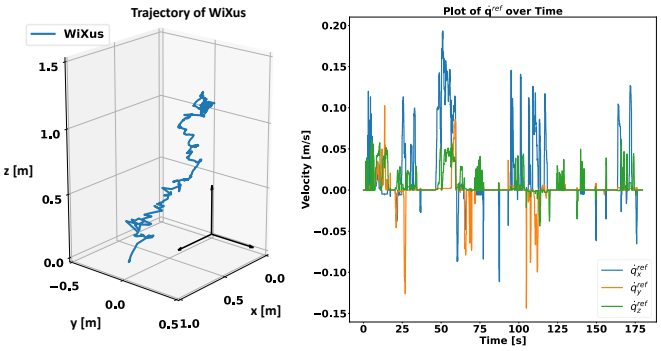

Fig. 18. Trajectory of WiXus and the corresponding time-series data of the commanded velocity. The results show WiXus following fine manual control commands to move through space.

between closing and opening. WiXus attaches the loppers to its body using the tool attachment wire, controls its whole-body posture including the loppers using the anchored wires, and controls the state of the loppers (closing/opening) using its wheeled-legs. This experiment demonstrates a new approach in which a wheeled-legged robot performs tool utilization that requires tool operation while suspended by wire-driven actuation.

V. Conclusion

In this study, we developed WiXus, a novel robot that integrates a wheeled-legged system and a wire-driven system, and conducted experiments to demonstrate its capabilities: a mapping experiment and a cliff climbing experiment for mobility capabilities, a rescue task experiment for object manipulation capability, and a harvesting experiment with loppers for tool utilization capability. WiXus is a two-wheeled-legged robot equipped with four wire winding modules for anchoring to the environment and one wire winding module for tool attachment. By using wire-driven actuation with wires anchored to the environment, WiXus frees its wheeled-legs from the roles of locomotion, and the experimental results confirm that this enhances the task execution capability of the wheeled-legs. Therefore, this study demonstrates that the approach of environmental anchoring with wire-driven actuation can expand the operational domain of wheeled-legged robots.

While the demonstrations involve partial operator input, they represent an initial step to validate the feasibility of the proposed concept, which can be extended to autonomous task execution by integrating environmental perception and motion planning. As a future direction, WiXus could plan its own motions to accomplish tasks based on the given environment and tools. If WiXus can autonomously perform motion planning with its body that is capable of both locomotion and manipulation, it is expected to accomplish more complex and diverse tasks.

References

[1] M. Bjelonic, R. Grandia, O. Harley, C. Galliard, S. Zimmermann, and M. Hutter, "Whole-Body MPC and Online Gait Sequence Generation for Wheeled-Legged Robots," in *Proceedings of the 2021 IEEE/RSJ International Conference on Intelligent Robots and Systems*, 2021, pp. 8388–8395.

[2] J. Lee, M. Bjelonic, A. Reske, L. Wellhausen, T. Miki, and M. Hutter, "Learning robust autonomous navigation and locomotion for wheeled-legged robots," *Science Robotics*, vol. 9, no. 89, p. eadi9641, 2024.

[3] C. Zhang, T. Liu, S. Song, and M. Q.-H. Meng, "System Design and Balance Control of a Bipedal Leg-wheeled Robot," in *Proceedings of the 2019 IEEE International Conference on Robotics and Biomimetics*, 2019, pp. 1869–1874.

[4] T. Liu, C. Zhang, S. Song, and M. Q.-H. Meng, "Dynamic Height Balance Control for Bipedal Wheeled Robot Based on ROS-Gazebo," in *Proceedings of the 2019 IEEE International Conference on Robotics and Biomimetics*, 2019, pp. 1875–1880.

[5] Z. Yang, Z. Bian, and W. Zhang, "Design and control of multi-mode wheeled-bipedal robot with parallel mechanism," in *2023 International Conference on Communications, Computing and Artificial Intelligence (CCCAI)*, 2023, pp. 69–74.

[6] V. Klemm, A. Morra, C. Salzmann, F. Tschopp, K. Bodie, L. Gulich, N. Kng, D. Mannhart, C. Pfister, M. Vierneisel, F. Weber, R. Deuber, and R. Siegwart, "Ascento: A Two-Wheeled Jumping Robot," in *Proceedings of the 2019 IEEE International Conference on Robotics and Automation*, 2019, pp. 7515–7521.

[7] "TITA (Direct Drive Technology)," https://shop.directdrive.com/products/tita.

[8] "DIABOLO (Direct Drive Technology)," https://shop.directdrive.com/products/diablo-world-s-first-direct-drive-self-balancing-wheeled-leg-robot.

[9] "Go2-W (Unitree Robotics)," https://www.unitree.com/go2-w.

[10] "B2-W (Unitree Robotics)," https://www.unitree.com/b2-w.

[11] "Handle (Boston Dynamics)," https://robotsguide.com/robots/handle.

[12] X. Li, H. Zhou, H. Feng, S. Zhang, and Y. Fu, "Design and Experiments of a Novel Hydraulic Wheel-Legged Robot (WLR)," in *Proceedings of the 2018 IEEE/RSJ International Conference on Intelligent Robots and Systems*, 2018, pp. 3292–3297.

[13] X. Li, H. Zhou, S. Zhang, H. Feng, and Y. Fu, "WLR-II, a Hose-less Hydraulic Wheel-legged Robot," in *Proceedings of the 2019 IEEE/RSJ International Conference on Intelligent Robots and Systems*, 2019, pp. 4339–4346.

[14] D. Bury, J.-B. Izard, M. Gouttefarde, and F. Lamiraux, "Continuous Collision Detection for a Robotic Arm Mounted on a Cable-Driven Parallel Robot," in *Proceedings of the 2019 IEEE/RSJ International Conference on Intelligent Robots and Systems*, 2019, pp. 8097–8102.

[15] L. L. Cone, "Skycam-an aerial robotic camera system," *Byte*, vol. 10, no. 10, p. 122, 1985.

[16] T. Miki, P. Khrapchenkov, and K. Hori, "UAV/UGV Autonomous Cooperation: UAV assists UGV to climb a cliff by attaching a tether," in *Proceedings of the 2019 IEEE International Conference on Robotics and Automation*, 2019, pp. 8041–8047.

[17] S. Inoue, K. Kawaharazuka, T. Suzuki, S. Yuzaki, K. Okada, and M. Inaba, "CubiX: Portable Wire-Driven Parallel Robot Connecting to and Utilizing the Environment," in *Proceedings of the 2024 IEEE/RSJ International Conference on Intelligent Robots and Systems*, 2024, pp. 1296–1301.

[18] S. Inoue, K. Kawaharazuka, T. Suzuki, S. Yuzaki, K. Okada, and M. Inaba, "Overcoming Physical Limitations Utilizing the Surrounding Environment with a Wire-Driven Multipurpose Robot," *Advanced Robotics Research*, vol. 1, no. 1, p. 202400021.

[19] S. Inoue, K. Kawaharazuka, K. Yoneda, S. Yuzaki, Y. Sahara, T. Suzuki, and K. Okada, "An RGB-D Camera-Based Multi-Small Flying Anchors Control for Wire-Driven Robots Connecting to the Environment," in *Proceedings of the 2025 IEEE/RSJ International Conference on Intelligent Robots and Systems*, 2025, pp. 20 442–20 447.

[20] M. Labbé and F. Michaud, "RTAB-Map as an open-source lidar and visual simultaneous localization and mapping library for large-scale and long-term online operation," *Journal of Field Robotics*, vol. 36, no. 2, pp. 416–446, 2019.

[21] J. Bohren and S. Cousins, "The SMACH High-Level Executive [ROS News]," *IEEE Robotics Automation Magazine*, vol. 17, no. 4, pp. 18–20, 2010.